MALARIA

# The cytoplasmic prolyl-tRNA synthetase of the malaria parasite is a dual-stage target of febrifugine and its analogs

Jonathan D. Herman,[1,2,3,4,5]* Lauren R. Pepper,[6]* Joseph F. Cortese,[1] Guillermina Estiu,[7,8]† Kevin Galinsky,[1] Vanessa Zuzarte-Luis,[9] Emily R. Derbyshire,[10] Ulf Ribacke,[2] Amanda K. Lukens,[1,2] Sofia A. Santos,[11,12] Vishal Patel,[10] Clary B. Clish,[1] William J. Sullivan Jr.,[13] Huihao Zhou,[14] Selina E. Bopp,[2] Paul Schimmel,[14,15] Susan Lindquist,[6,16] Jon Clardy,[1,10] Maria M. Mota,[9] Tracy L. Keller,[17] Malcolm Whitman,[17] Olaf Wiest,[7,8,18] Dyann F. Wirth,[1,2]‡ Ralph Mazitschek[1,2,11]‡

**The emergence of drug resistance is a major limitation of current antimalarials. The discovery of new druggable targets and pathways including those that are critical for multiple life cycle stages of the malaria parasite is a major goal for developing next-generation antimalarial drugs. Using an integrated chemogenomics approach that combined drug resistance selection, whole-genome sequencing, and an orthogonal yeast model, we demonstrate that the cytoplasmic prolyl–tRNA (transfer RNA) synthetase (*Pf*cPRS) of the malaria parasite *Plasmodium falciparum* is a biochemical and functional target of febrifugine and its synthetic derivative halofuginone. Febrifugine is the active principle of a traditional Chinese herbal remedy for malaria. We show that treatment with febrifugine derivatives activated the amino acid starvation response in both *P. falciparum* and a transgenic yeast strain expressing *Pf*cPRS. We further demonstrate in the *Plasmodium berghei* mouse model of malaria that halofuginol, a new halofuginone analog that we developed, is active against both liver and asexual blood stages of the malaria parasite. Halofuginol, unlike halofuginone and febrifugine, is well tolerated at efficacious doses and represents a promising lead for the development of dual-stage next-generation antimalarials.**

## INTRODUCTION

Almost one-third of the world's population is exposed to malaria, with the highest burden of disease found in low-income nations in Asia, South America, and Africa. The World Health Organization estimates that malaria parasites infect more than 200 million people each year, killing about 600,000 people—mostly young children and pregnant women in sub-Saharan Africa—whereas many more suffer permanent disabilities (*1*).

The causative agents of malaria are protozoan parasites of the genus *Plasmodium* that are transmitted between human hosts by mosquitoes. In humans, parasites progress through a liver stage, an asexual symptomatic stage, and a sexual blood stage. The emergence and spread of clinical resistance to mainstay drugs, including artemisinin and its derivatives, is the major limitation of current antimalarial drugs (*2*–*4*). Developing therapies that act on unexploited vulnerabilities in the *Plasmodium* parasite is necessary for renewed worldwide efforts to ultimately eradicate malaria (*5*). Thus, the discovery not only of new chemical classes of potential antimalaria compounds but also of new druggable targets and pathways is essential (*6*).

To address this need, we chose to target the cytoplasmic prolyl–tRNA (transfer RNA) synthetase (*Pf*cPRS) of *Plasmodium falciparum* based on our previous work demonstrating that the natural product febrifugine and its synthetic derivative halofuginone (Fig. 1A) potently inhibit activity of the bifunctional glutamyl-prolyl-tRNA synthetase (EPRS) of mammalian cells (*7*). Aminoacyl-tRNA synthetases are validated targets in several microorganisms and have more recently been proposed as attractive targets for chemotherapeutic intervention in malaria (*8*–*14*).

The natural product febrifugine constitutes the curative ingredient of an ancient Chinese herbal remedy that has been used for over 2000 years for the treatment of fevers and malaria (*15*–*17*). However, poor tolerability has precluded the clinical development of either febrifugine or its synthetic derivative halofuginone for the treatment of malaria (*17*). Thus, our aims were to elucidate the molecular basis of the antiparasitic activity of febrifugine analogs and to identify derivatives with improved tolerability that could serve as a starting point for rational drug development.

The tRNA synthetase machinery differs greatly between humans and *P. falciparum*. In humans, EPRS is the only enzyme with PRS activity and forms the central framework of a multisubunit complex that is involved in a diverse number of biological processes in addition to its canonical synthetase activity (*18*). In contrast, *P. falciparum*

[1]Infectious Diseases Program, Broad Institute, Cambridge, MA 02142, USA. [2]Department of Immunology and Infectious Diseases, Harvard T.H. Chan School of Public Health, Boston, MA 02115, USA. [3]Biological and Biomedical Sciences, Boston, MA 02115, USA. [4]Harvard/Massachusetts Institute of Technology (MIT) Division of Health Sciences and Technology, Boston, MA 02115, USA. [5]Harvard/MIT MD-PhD Program, Harvard Medical School, Boston, MA 02115, USA. [6]Whitehead Institute for Biomedical Research, Cambridge, MA 02142, USA. [7]Department of Chemistry and Biochemistry, University of Notre Dame, Notre Dame, IN 46556, USA. [8]Center for Rare and Neglected Diseases, University of Notre Dame, Notre Dame, IN 46556, USA. [9]Instituto de Medicina Molecular, Faculdade de Medicina, Universidade de Lisboa,1649-028 Lisbon, Portugal. [10]Department of Biological Chemistry and Molecular Pharmacology, Harvard Medical School, Boston, MA 02115, USA. [11]Center for Systems Biology, Massachusetts General Hospital, Boston, MA 02114, USA. [12]Instituto de Investigação do Medicamento (iMed.ULisboa), Faculdade de Farmácia, Universidade de Lisboa, Av. Professor Gama Pinto, Lisbon 1640-003, Portugal. [13]Departments of Pharmacology and Toxicology and Microbiology and Immunology, Indiana University School of Medicine, Indianapolis, IN 46202, USA. [14]Department of Molecular Biology, Skaggs Institute for Chemical Biology, The Scripps Research Institute, La Jolla, CA 92037, USA. [15]The Scripps Research Institute, Florida, Jupiter, FL 33458, USA. [16]Howard Hughes Medical Institute, Department of Biology, MIT, Cambridge, MA 02139, USA. [17]Department of Developmental Biology, Harvard School of Dental Medicine, Boston, MA 02115, USA. [18]School of Chemical Biology and Biotechnology, Laboratory for Computational Chemistry and Drug Design, Peking University Shenzhen Graduate School, Shenzhen 518055, China.
*These authors contributed equally to this work
†Deceased May 9, 2014.
‡Corresponding author. E-mail: rmazitschek@mgh.harvard.edu (R.M.); dfwirth@hsph.harvard.edu (D.F.W.)

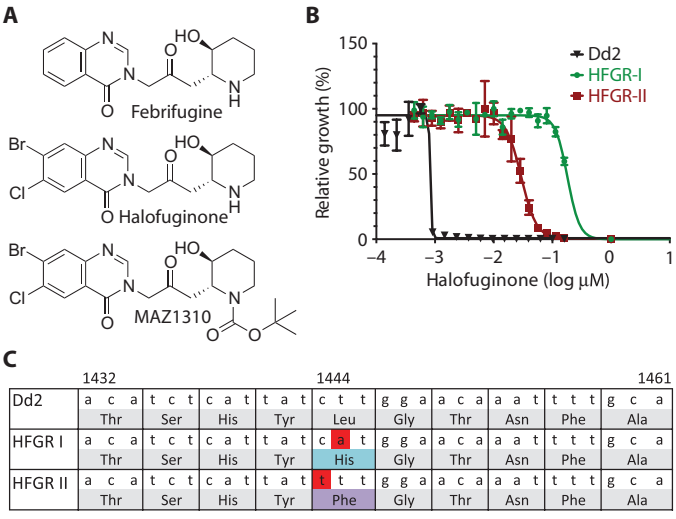


**Fig. 1. *Pfc*PRS of *P. falciparum* is the target of halofuginone.** (**A**) Shown are chemical structures for febrifugine and its analogs halofuginone (relative stereochemistry) and MAZ1310 (relative stereochemistry). (**B**) Independent selection experiments under intermittent and dose-adjusted drug pressure starting with the Dd2 laboratory strain of *P. falciparum* yielded two highly resistant clones (HFGR-I and HFGR-II). (**C**) Whole-genome sequencing identified nonsynonymous mutations in the highly resistant clones HFGR-I and HFGR-II that map to the same amino acid codon, $L^{482}$, in *Pfc*PRS (PF3D7_1213800).

expresses two putative PRS enzymes, one that acts in the apicoplast (PfaPRS, PF3D7_0925300) and one that acts in the cytoplasm (PfcPRS, PF3D7_1213800) (*19*). Because of the difference in tRNA synthetase machinery and the large evolutionary distance between humans and *P. falciparum*, we selected an unbiased approach to identify the target of febrifugine derivatives in *P. falciparum*.

Here, we report the validation of *Pfc*PRS as the functional target of febrifugine analogs. We identify halofuginol as a new halofuginone analog that may be a promising lead compound with potent in vivo efficacy against the liver and blood stages of the mouse malaria parasite *Plasmodium berghei*.

## RESULTS

### The *Pfc*PRS of *P. falciparum* is a molecular target of febrifugine and its analogs

To identify the molecular target, we chose the select-sequence experimental design in which we selected in vitro drug-resistant *P. falciparum* parasites and sequenced their genomes to identify genetic mutations in *P. falciparum* associated with resistance to febrifugine and its analogs (*20*, *21*). We carried out resistance selections in the wild-type Dd2 strain of *P. falciparum* exposed to halofuginone [median effective concentration ($EC_{50}$) = 0.5 nM], resulting in two highly resistant parasite lines that were independently selected: HFGR-I (halofuginone resistant line I; $EC_{50}$ = 180 nM) and HFGR-II ($EC_{50}$ = 30 nM) (Fig. 1B) (*22*). Both resistant strains were found to be cross-resistant to febrifugine (table S1).

To identify the genetic loci that contribute to halofuginone resistance, we sequenced the full genome of the HFGR-I and HFGR-II *P. falciparum* strains along with the parental Dd2 strain (*23*, *24*). The only gene with nonsynonymous single-nucleotide polymorphisms (SNPs) identified in both resistant lines was PF3D7_1213800, which was annotated as a putative cytoplasmic proline aminoacyl-tRNA synthetase that resembled the *P. falciparum* PRS isoform with closest homology to the human ortholog (*19*). The independently selected mutations T1445A and C1444T occurred in the same codon of *Pfc*PRS (Fig. 1C) translating into an L482H (HFGR-I) and L482F (HFGR-II) amino acid change. Both SNPs were independently confirmed by high-resolution melting genotyping (fig. S1) and were verified by Sanger sequencing (*25*). None of the SNPs identified through our selection experiments corresponded to any of the nine nonsynonymous SNPs in PF3D7_1213800 that are cataloged in PlasmoDB in naturally occurring *P. falciparum* strains (*26*). These data are consistent with our observation that halofuginone is equally active in a panel of 31 representative *P. falciparum* clinical isolates with diverse drug resistance profiles (fig. S2). These results suggest that *Pfc*PRS may be the primary target of halofuginone and febrifugine. This possibility was further supported by the observation that addition of exogenous proline to the in vitro culture medium of *P. falciparum* increased the $EC_{50}$ of halofuginone in a concentration-dependent manner, although only ~3-fold shift in inhibition was observed after a 50-fold increase in proline concentration in the culture medium (fig. S3).

### Replacement of yeast PRS by *Pfc*PRS confers sensitivity to halofuginone in yeast

To validate *Pfc*PRS as the functional target of halofuginone, we used a yeast transgenic system. The PRS of the yeast *Saccharomyces cerevisiae* (*Sc*PRS, YHR020w) is similar to *Pfc*PRS. However, we discovered that *S. cerevisiae* was not sensitive to halofuginone. This allowed us to use yeast as an orthogonal model for both target confirmation of halofuginone and validation of the resistance phenotype of the mutant alleles identified in our drug resistance selections (Fig. 2).

First, we performed a complementation test of *Pfc*PRS in *S. cerevisiae*. We found that episomal expression of *Pfc*PRS could complement deletion of the chromosomal copy of *Sc*PRS, an essential gene and the only locus that encodes a PRS in *S. cerevisiae*. Next, we generated transgenic yeast strains that would episomally express only *Sc*PRS or only *Pfc*PRS (Fig. 2A). Whereas both strains exhibited comparable growth characteristics, only the *Pfc*PRS-expressing strain displayed a dose-dependent sensitivity to halofuginone treatment (Fig. 2B and fig. S4), which was attenuated by addition of free L-proline (fig. S5).

To validate the resistance allele L482H, we also generated a yeast strain expressing L482H *Pfc*PRS (Fig. 2A). This strain was viable both in the presence and absence of halofuginone consistent with the L482H mutation conferring resistance to halofuginone (Fig. 2B). Similar activity was observed for the L482F mutant, whereas none of the tested yeast strains were susceptible to inhibition by the control compound MAZ1310 (Fig. 1A), a halofuginone analog that does not bind to PRS (*7*, *27*). These results, together, confirmed that *Pfc*PRS is the functional target of febrifugine and halofuginone and that mutation of amino acid 482 in *Pfc*PRS conferred resistance to febrifugine and halofuginone.

### Febrifugine and halofuginone induce the amino acid starvation response in *P. falciparum*

After validation of *Pfc*PRS as a molecular target of febrifugine and its analogs, we next investigated how halofuginone dysregulates the

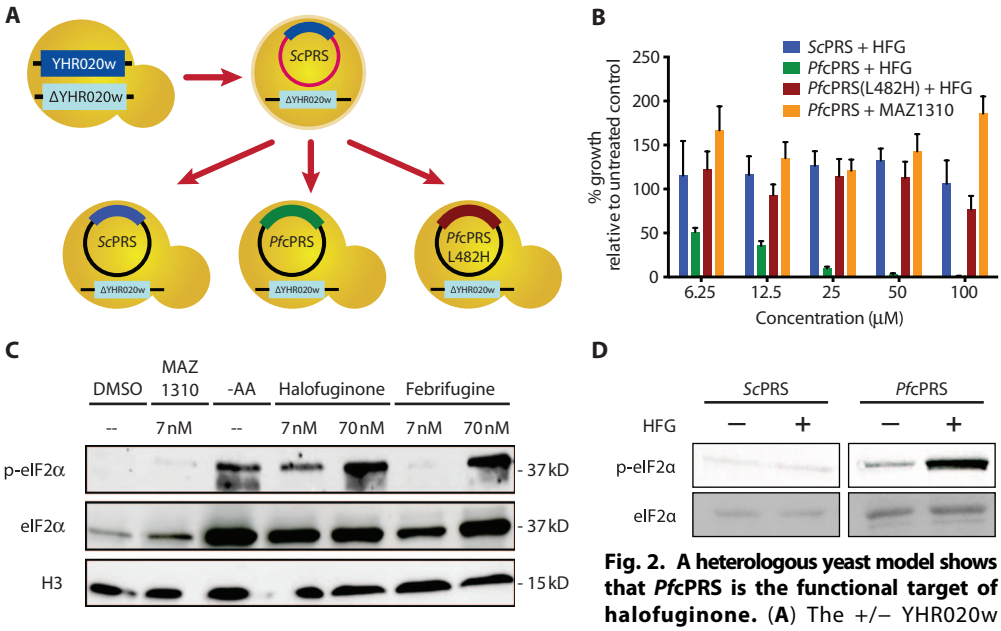


**Fig. 2. A heterologous yeast model shows that *Pfc*PRS is the functional target of halofuginone.** (**A**) The +/− YHR020w (*ScPRS*) heterozygous strain of *S. cerevisiae* was transformed with a YHR020w-containing plasmid, and haploid spores were selected for genomic deletion of YHR020w. The intermediate strain was transformed with a second plasmid with an orthogonal selection marker and YHR020w, wild-type *Pfc*PRS (codon-optimized) or mutant *Pfc*PRS (codon-optimized), and was subsequently selected for loss of the first plasmid. (**B**) Only transgenic *S. cerevisiae* expressing wild-type *Pfc*PRS (green) displayed dose-dependent sensitivity to halofuginone, whereas strains expressing *Sc*PRS (blue) or the L482H *Pfc*PRS mutant (red) were insensitive to halofuginone treatment up to 100 μM (all strains were pdr1,3-deleted). The control compound MAZ1310 did not affect growth of *Pfc*PRS expressing yeast (orange). (**C**) Halofuginone or febrifugine treatment or amino acid starvation (–AA) induced phosphorylation of eIF2α (p-eIF2α) after 90 min. Western blot analysis of phosphorylated eIF2α and total eIF2α protein in drug-treated asynchronous Dd2 *P. falciparum* cultures is shown. Histone H3 is the loading control, and the blot is representative of two independent replicates. (**D**) Halofuginone (HFG) treatment induced pronounced eIF2α phosphorylation in *Pfc*PRS but not in *Sc*PRS-expressing *S. cerevisiae*.

amino acid sensing mechanism in the parasite. In mammalian cells, inhibition of EPRS by halofuginone or direct amino acid deprivation results in phosphorylation of the eukaryotic initiation factor 2α (eIF2α) and consequent activation of the amino acid response (AAR) pathway (fig. S6) (*7*, *28*). Recent research has confirmed the existence of a functional AAR in the intraerythrocytic stage of *P. falciparum* and has demonstrated induction of phosphorylated eIF2α in response to amino acid starvation (*13*, *29*).

To probe for the activation of the AAR, we treated asynchronous *P. falciparum* Dd2 cultures with halofuginone, febrifugine, or MAZ1310 as a negative control and quantified the amount of eIF2α and phosphorylated eIF2α by Western blot analysis compared to amino acid deprivation. Halofuginone and febrifugine treatment increased eIF2α phosphorylation in a dose-dependent manner that was comparable to eIF2α phosphorylation during amino acid starvation (Fig. 2C and fig. S7). Dimethyl sulfoxide and MAZ1310 control treatments failed to increase eIF2α phosphorylation.

Next, we investigated the effect of halofuginone treatment on eIF2α phosphorylation in yeast strains expressing *Pfc*PRS or *Sc*PRS. Only the halofuginone-sensitive *Pfc*PRS-expressing strain exhibited robust induction of phosphorylated eIF2α in response to exposure to the compound (Fig. 2D), whereas no difference in eIF2α phosphorylation was observed in the *Sc*PRS-expressing yeast strain. These results, together, demonstrate that halofuginone treatment induced the amino acid starvation pathway through direct inhibition of *Pfc*PRS.

## Molecular characterization of the ligand-target interaction establishes mechanistic insights

To provide a structural rationale for the experimental results and to aid rational drug design efforts, we modeled the binding mode of the *Pfc*PRS to adenosine 5′-triphosphate (ATP) and halofuginone based on the recently published structure of the ternary human PRS complex [Protein Data Bank (PDB): 4HVC] (*30*). Our model showed that the N-protonated hydroxypiperidine moiety of halofuginone was stabilized by a network of hydrogen bond interactions (Fig. 3A), which were not formed by MAZ1310. The interactions between halofuginone, ATP, and *Pfc*PRS were similar to the binding mode observed for human PRS consistent with the similarity of the *Pfc*PRS core catalytic domains. These results show that halofuginone is a competitive inhibitor of the proline and tRNA binding sites of *Pfc*PRS (*30*).

Within the core class II catalytic domains, *Sc*PRS shares 77 and 70% similarity with human and *Plasmodium* enzymes, respectively (fig. S8). Comparison of *Pfc*PRS to *Sc*PRS provided insights into the unexpected differential activity of halofuginone in *P. falciparum* and *S. cerevisiae*. Although the active site residues that interact with halofuginone were identical in both organisms, molecular dynamics simulations revealed the origin of the experimentally observed insensitivity of *S. cerevisiae Sc*PRS, which was not recognized by halofuginone in a standard docking approach. Unlike *Pfc*PRS, the geometry of the ternary *Sc*PRS-halofuginone-ATP complex was not stable, resulting in significant structural rearrangement of several amino acid side chains and the reorientation of the quinazoline moiety of halofuginone (compare Fig. 3A with 3B). We speculated that the structural change may be attributable to a threonine-to-serine mutation in position 512 (numbering based on *Pfc*PRS). $T^{512}$ is conserved in the PRS of all halofuginone-sensitive apicomplexan parasites, and also in the EPRS of mouse and human. The presence of $S^{512}$ in the yeast PRS resulted in a slightly altered binding mode for adenosine, which in turn impacted the halofuginone-ATP interaction and consequently altered the orientation of halofuginone (Fig. 3B). The critical role of ATP for halofuginone binding is consistent with our previous finding that ATP is required for tight binding of halofuginone to human EPRS (*7*, *30*). Furthermore, Hwang and Yogavel have recently solved the structures of free human EPRS and *Pfc*PRS, respectively, demonstrating significant conformational changes in the apoenzyme (*31*, *32*).

Next, we investigated the L482H *Pfc*PRS mutant to understand the experimentally observed decreased sensitivity of this mutant to

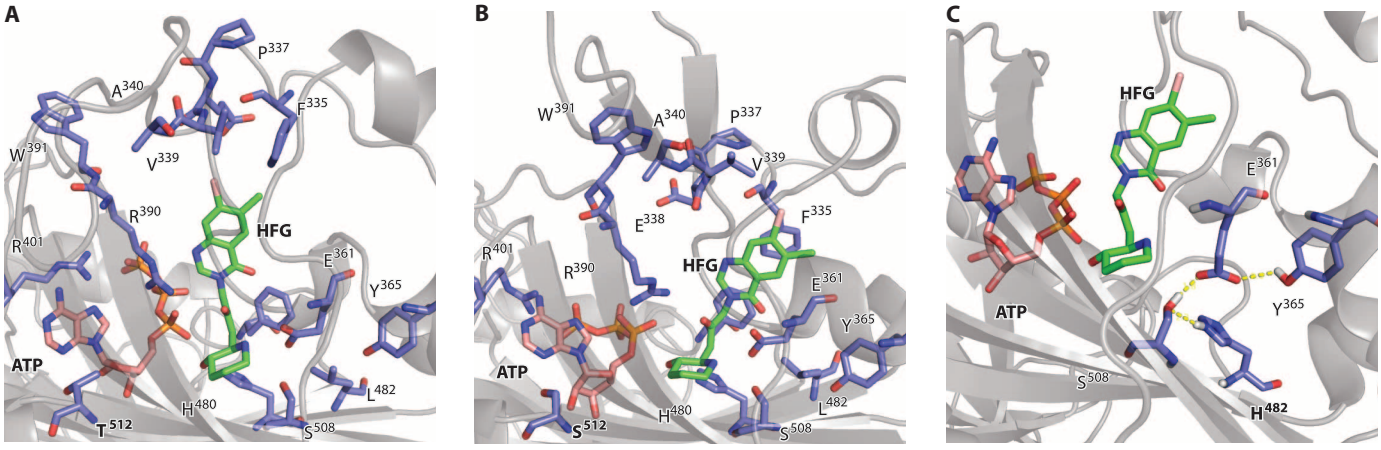


**Fig. 3. Models of the ternary complex of PRS with ATP and halofuginone.** (**A** to **C**) Molecular dynamics simulations of the ternary complex of PRS with ATP and halofuginone for (A) the *Pfc*PRS of *P. falciparum*, (B) the *Sc*PRS of *S. cerevisiae*, and (C) the *Pfc*PRS L482H mutant of *P. falciparum*. The differential binding affinity of halofuginone to *Pfc*PRS and *Sc*PRS can be traced to a T512S mutation in *Sc*PRS that results in a differential ATP-binding geometry. This modification in turn changes the interaction of ATP with halofuginone and results in a reorientation of the loop consisting of residues 318 to 337. Specifically, $F^{335}$, which stacks against the aromatic ring of halofuginone, is in a different position in the two structures. Additionally, the position of the triphosphate is different, which in turn changes the orientation of $Arg^{401}$. (C) Effect of the L482H resistance mutation on the interactions of halofuginone in the active site of *Pfc*PRS. $Leu^{482}$ is adjacent to the proline-binding pocket, and although it does not directly participate in the hydrogen bond network formed between halofuginone and *Pfc*PRS, it does support the binding geometry of the amino acid residues that directly interact with halofuginone. The histidine in the L482H mutant provides an alternative hydrogen bond acceptor, thus destabilizing the network. All residues are numbered on the basis of *Pfc*PRS.

halofuginone. $L^{482}$ is adjacent to the proline-binding pocket and did not directly interact with either halofuginone or proline. However, our molecular dynamics simulations revealed that $E^{361}$ moves from a position where it interacts with halofuginone (Fig. 3C) to a position where it interacts with $S^{508}$ and $Y^{365}$. We hypothesized that this structural change was due to the hydrogen bond that the mutant $H^{482}$ residue established with $S^{508}$, thus reorienting $S^{508}$ such that it formed a hydrogen bond with $E^{361}$. The experimental observation that the L482H mutant is less strongly inhibited by halofuginone underscored the critical importance of this interaction. The L482F mutation observed in the other resistant parasite line in contrast induced steric repulsion with residues nearby, disrupting the interactions in the binding pocket (fig. S9). The results of our molecular dynamics simulations were consistent with the biological activity of halofuginone and established a detailed mechanistic explanation for the $L^{482}$ resistance mutations and the unexpected insensitivity of *Sc*PRS, both of which were difficult to rationalize by standard molecular docking approaches.

## Halofuginol is active against the asexual erythrocytic and liver stages of *P. falciparum* in vitro

Dose-limiting toxicity, rather than lack of efficacy, has precluded clinical development of febrifugine and its analogs such as halofuginone as antimalarial drugs (*17*). We speculated that the observed side effects of halofuginone and febrifugine could, at least in part, be independent from inhibition of the human PRS. We proposed that the off-target effects may originate from the ability of the compounds to epimerize in solution through formation of a reactive intermediate enabled by the central ketone common to febrifugine and halofuginone (fig. S10) (*33*). Previously reported efforts to remove this functionality resulted in loss of activity (*34*). We reasoned that formal reduction of the ketone to yield a secondary alcohol would eliminate the ability to form a reactive Michael acceptor, while retaining the functionality to form the critical hydrogen bonds within the target complex. Introduction of the alcohol also introduced an additional stereocenter. We therefore established synthetic approaches to access both epimers (Fig. 4A). (*7*, *34*).

Both compounds were tested for in vitro activity against the asexual blood stage of the *P. falciparum* 3D7 parasite strain. One epimer, halofuginol, demonstrated low nanomolar potency ($EC_{50}$ = 5.8 nM) comparable to febrifugine ($EC_{50}$ = 4.0 nM), whereas the other diastereomer, epi-halofuginol, was about 700-fold less active than halofuginone (Fig. 4B). As expected, the principle activity was attributable to one enantiomer, (*2′S,2R,3S*)-halofuginol, with the same absolute configuration of the piperidyl substituent as febrifugine and the active enantiomer of halofuginone (table S1) (*35*).

Cytotoxicity profiling in primary mouse embryonic fibroblasts ($EC_{50}$ = 373 nM) revealed that halofuginol was about 65 times more selective for *P. falciparum*. Halofuginol had similar activity ($EC_{50}$ = 14 nM) to halofuginone ($EC_{50}$ = 17 nM) in the in vitro *P. berghei* ANKA liver-stage model (Fig. 4C) (*36*). As expected, the activity profile of halofuginol in the HFGR parasite lines and in the transgenic *Pfc*PRS yeast strains was comparable to that of halofuginone (fig. S11). In addition, treatment of *P. falciparum* with halofuginol in vitro resulted in the phosphorylation of eIF2α in a similar manner to that observed with halofuginone (fig. S12, A and B).

Furthermore, in biochemical studies, we demonstrated that the affinity of halofuginol for mutant *Pfc*PRS ($K_i$ = 1120 ± 94.4 nM) was about 16-fold less compared to the wild-type enzyme ($K_i$ = 71.1 ± 9.0 nM). In addition, we found that the L482H resistance mutation also resulted in a 6.4-fold decreased affinity for proline [$K_{m(wt)}$ = 117.0 ± 11.2 μM and $K_{m(L482H)}$ = 747.7 ± 36.5 μM]. The biochemical characterization of human EPRS revealed virtually identical affinities for halofuginol ($K_i$ = 65.7± 6.3 nM) and proline ($K_m$ = 135.4 ± 9.8 μM) compared to wild-type *Pfc*PRS.

These results, together, are consistent with our hypothesis that reduction of the central ketone to eliminate the undesired ability to form a reactive Michael acceptor, while preserving the hydrogen bond

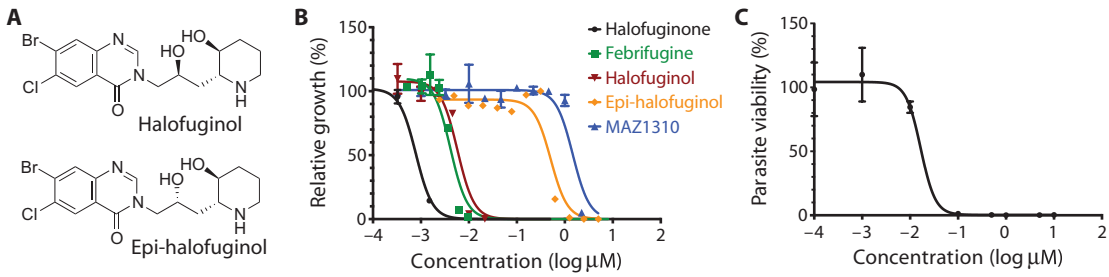


**Fig. 4. Halofuginol is active against the asexual erythrocytic and liver stages of the malaria parasite in vitro.** (**A**) Chemical structures of halofuginol (relative stereochemistry) and epi-halofuginol (relative stereochemistry). (**B**) In vitro activity of halofuginone, febrifugine, MAZ1310, halofuginol, and epi-halofuginol against *P. falciparum* strain 3D7 erythrocytic-stage parasites. Growth inhibition was quantified after 72 hours by staining with SYBR Green stain. (**C**) In vitro dose response for halofuginol after treatment of HepG2 cells with luciferase-expressing *P. berghei* ANKA liver-stage parasites.

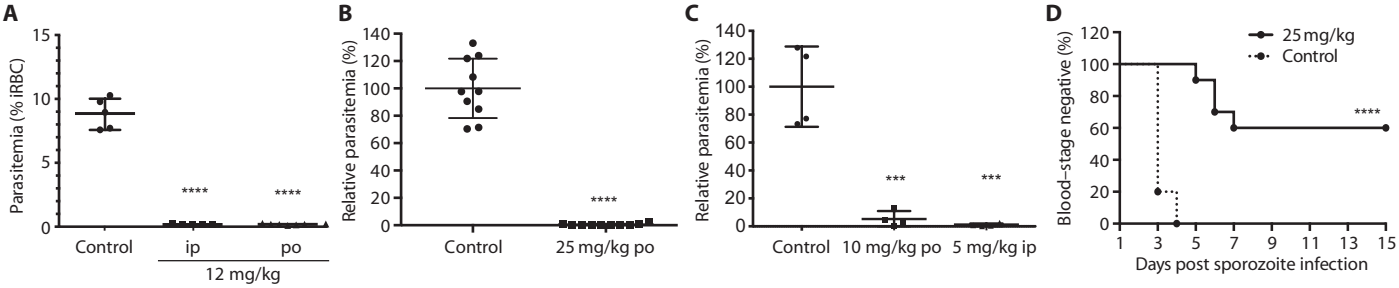


**Fig. 5. Halofuginol is active against the asexual erythrocytic and liver stages of the malaria parasite in vivo.** (**A**) Blood parasitemia at day 5 after infection in mice treated with halofuginol (ip in saline, $n = 5$; po in water, $n = 7$; or vehicle, $n = 5$) once a day for 4 and 10 days, respectively. Treatment with halofuginol began 24 hours after inoculation with $10^6$ red blood cells infected with green flourescent protein (GFP)–expressing *P. berghei* ANKA parasites. Blood parasite numbers were analyzed by fluorescence-activated cell sorting (FACS). (**B**) In vivo potency of halofuginol in the *P. berghei* mouse model of malaria. Shown is the relative parasitemia in mouse liver 44 hours after infection with luciferase-expressing *P. berghei* sporozoites. Mice were treated 1 hour after infection with halofuginol (25 mg/kg po) or vehicle [10% hydroxypropyl-β-cyclodextrin in 100 mM (pH 5.0) citrate buffer]. Parasite load was quantified relative to vehicle control by luminescence measurements. Data are displayed as means relative to vehicle-treated control, with the mean of the control group set to 100% ($n = 10$). (**C**) Relative parasitemia in mouse livers 44 hours after infection with *P. berghei* sporozoites. Mice were treated 1 hour after infection with halofuginol (ip in saline, po in water, $n = 4$). Parasite load was quantified relative to vehicle control by quantitative reverse transcription polymerase chain reaction (qRT-PCR) of *P. berghei* 18*S* ribosomal RNA (rRNA). Data are displayed as means relative to vehicle-treated control, with the mean of the control group set to 100%. (**D**) Mice were maintained for 14 days after infection or until they developed blood-stage malaria. Significance values (***$P < 0.001$, ****$P < 0.0001$) were calculated (GraphPad PRISM) by ordinary one-way analysis of variance (ANOVA) (A to C) and log-rank (Mantel-Cox) test (D). See tables S2 to S4 for detailed statistics. iRBC, infected red blood cells.

acceptor capacity, would result in reduced cytotoxicity in mammalian cells while retaining on-target activity in *Plasmodium* spp.

### Halofuginol is efficacious in vivo

To further assess halofuginol in an in vivo system, we used an adapted version of Peters' suppressive test (*37*, *38*) in a *P. berghei* mouse model of malaria. We found that halofuginol dosed daily at 12 mg/kg orally over 4 days reduced *P. berghei* parasite burden >99% by day 5 relative to control untreated mice that had an average parasitemia of 8.9% (Fig. 4D). Similar results were observed for intraperitoneal (ip) administration of halofuginol at 12 mg/kg once a day for 10 days (Fig. 4D). Both treatment strategies were very well tolerated and did not induce any adverse effects or gross pathological changes such as diarrhea, gastrointestinal hemorrhages/lesions, or discoloration of liver and spleen, which are the principle limiting toxicities observed with febrifugine and halofuginone treatment at efficacious doses (*17*). However, neither dosing strategy resulted in a sterilizing cure, and parasites recrudesced after discontinuation of drug treatment.

We next investigated the in vivo activity of halofuginol in a *P. berghei* sporozoite challenge model (*38*). As shown in Fig. 5A, halofuginol reduced the load of liver-stage parasites by >99% (at 46 hours after infection) after oral administration of a single 25 mg/kg dose, which we had established as a safe single-dose treatment; treatment with 5 mg/kg ip or 10 mg/kg po (per os) halofuginol reduced parasite burden by 99 and 95%, respectively (Fig. 5B). Mice treated at 25 mg/kg po were maintained for 14 days after infection or until they developed blood-stage malaria. All mice in the control group developed blood-stage malaria by day 4, whereas development of blood-stage malaria was delayed in the treated group and 60% of the test animals were considered cured after 2 weeks (Fig. 5, C and D). None of the treated animals displayed signs of adverse drug reactions (fig. S13). Separately, we tested halofuginone in the same *P. berghei* sporozoite challenge model and demonstrated that halofuginone is also efficacious in reducing liver-stage infection (fig. S14). However, at efficacious doses, we observed pronounced gastrointestinal toxicities (four of five) and lethality (one of five), similar to reports evaluating halofuginone for in vivo blood-stage activity (*17*). These results are consistent with the reduced cytotoxicity of halofuginol in vitro and support our hypothesis that chemical modification of the central ketone improves tolerability while retaining antimalarial activity in vivo.

## DISCUSSION

Developing therapies that act on unexploited vulnerabilities in the *Plasmodium* parasite will be necessary for renewed worldwide efforts

to eradicate malaria (*5*). Febrifugine was identified more than 60 years ago as the active principle of one of the oldest known antimalarial herbal remedies (*16*). However, poor tolerability prevented the clinical use of febrifugine as a mainstay antimalarial, and previous medicinal chemistry efforts failed to identify viable alternatives (*17*).

We set out to address two issues: First, we sought to identify the functional target of febrifugine and its derivatives in *P. falciparum* to facilitate rational drug development. Second, we sought to develop derivatives with reduced cytotoxicity in the human host.

Using an unbiased target identification approach, we report the identification and validation of *Pf*cPRS, one of two prolyl-tRNA synthetases encoded in the *Plasmodium* genome and show that *Pf*cPRS is the biochemical and functionally relevant target of febrifugine analogs. We support our findings by target validation in an orthogonal transgenic yeast model and provide a mechanistic rationale for drug action at a molecular level. We established that halofuginol, a new halofuginone analog previously developed by our group, had excellent in vivo activity in two *P. berghei* malaria mouse models against the liver stage and the asexual blood stage of the parasite. Dual-stage activity is essential for antimalarial drugs that will be used to eliminate malaria. However, in vivo activity against the liver stage of the malaria parasite by febrifugine derivatives has not been demonstrated before. Notably, we were able to show that a single oral dose of halofuginol (25 mg/kg) resulted in >99% reduction in liver parasites and an overall 60% cure rate in the *P. berghei* liver-stage model. Halofuginol was also highly efficacious against the asexual blood stage as demonstrated by >99% reduction in parasitemia after a 4-day oral treatment at 12 mg/kg, but failed to result in a sterile cure. At pharmaceutically efficacious concentrations, halofuginol was better tolerated than febrifugine and halofuginone and did not induce any adverse effects even after daily intraperitoneal administration at 12 mg/kg for 10 days.

Previous reports have suggested that tRNA synthetases represent attractive targets for the treatment of malaria (*8*–*13*, *39*). Recently, Winzeler and co-workers identified cladosporin, a fungal metabolite previously not known to have inhibitory activity against aminoacyl-tRNA synthetase, as a selective and specific inhibitor of the *P. falciparum* lysyl-tRNA synthetase with mid-nanomolar in vitro activity against blood- and liver-stage parasites (*14*). In addition, the isoleucyl-tRNA synthetase (IRS) inhibitor mupirocin and the isoleucine analog thiaisoleucine have been shown to target the apicoplast IRS and cytoplasmic IRS, respectively, and can kill blood-stage parasites at mid-nanomolar and low-micromolar concentrations (*13*). However, thiaisoleucine did not induce eIF2α phosphorylation, which is a sensitive indicator of the starvation response and a hallmark of isoleucine withdrawal, suggesting that the antiparasitic activity of thiaisoleucine is due to inhibition of secondary targets (*13*). An alternative explanation is that this could be the result of insufficient inhibition of IRS activity at the tested concentrations due to the short half-life or low potency of the compound.

In contrast, we show that febrifugine analogs induce eIF2α phosphorylation in *Plasmodium* parasites and transgenic yeast expressing *Pf*cPRS. This establishes a valuable chemical tool with which to study the amino acid starvation pathway in *P. falciparum* and *S. cerevisiae*, and also validates *Pf*cPRS as an attractive target for the development of new classes of antimalarials that are active against both the erythrocytic and liver stages of the malaria parasite. Additionally, the transgenic yeast strain reported here in combination with halofuginone could prove valuable for mechanistically dissecting nutrient deprivation signaling pathways in eukaryotes and to study the independence and interrelatedness of nutrient sensing by the AAR and the target of rapamycin (TOR) pathways (*40*).

We speculate that the broad-spectrum antiprotozoal activity of halofuginone could be due to conservation of PRS. Halofuginone is currently approved in veterinary medicine to treat coccidiosis in poultry (caused by *Eimeria tenella*) and cryptosporidiosis in cattle (caused by *Cryptosporidium parvum*) (*41*–*43*). Molecular phylogenetics of the catalytic domain confirms that *E. tenella* PRS and *C. parvum* PRS share 81 and 86% similarity with *Pf*cPRS, respectively (fig. S7). Furthermore, these agents may be effective against other human malaria parasites such as *Plasmodium vivax*, which shares 95% conservation of the active site of the *Pf*cPRS, and a wide swath of infectious diseases caused by protozoan parasites, including toxoplasmosis, babesiosis, and Chaga's disease.

The ability to generate and isolate *P. falciparum* lines that are genetically resistant to halofuginone was critical to our approach to identify and validate *Pf*cPRS as a target for malaria drug development. However, as is true for any antimalarial drug, resistance also constitutes a concern for potential clinical use of *Pf*cPRS inhibitors. Although our studies did not investigate the long-term stability and fitness costs of the identified resistance mutations in *P. falciparum* in the context of competing wild-type parasites, we are encouraged that all identified mutations in *Pf*cPRS mapped to the same amino acid codon, which suggests that mutational plasticity could be restricted for this target. Nonetheless, additional research is needed to investigate this issue in greater detail. In this context, it will also be of interest to identify drug combinations that synergize with *Pf*cPRS inhibitors.

Although our studies identify halofuginol as an attractive starting point for rational development of *Pf*cPRS inhibitors as next-generation antimalarials, detailed drug metabolism and pharmacokinetics studies will be needed to better understand the in vivo pharmacology of this compound and to guide future drug development. In particular, it will be important to understand the consequences of blocking human EPRS. *Pf*cPRS inhibitors with improved biochemical selectivity might be more attractive candidates for clinical development. Our next goal will be to focus on the development of such compounds. Combined with our recent identification of the human EPRS as the target of halofuginone, the computational and mechanistic studies presented here provide a detailed understanding of the ligand-protein interaction at atomic resolution in both the human and parasite enzymes, establishing a clear path forward to the design of new inhibitors with dual-stage activity that selectively target the malaria parasite.

## MATERIALS AND METHODS

### Study design

The objectives of this study were to identify and validate the target of febrifugine and its derivatives in *P. falciparum* and to assess their in vivo efficacy and tolerability in mouse models of liver- and blood-stage malaria. First, two HFGR lines were independently selected under intermittent drug pressure and sequenced. Whole-genome analysis identified *Pf*cPRS (PF3D7_1213800) as the only gene with mutations in both strains. Next, *Pf*cPRS was validated as a mechanistic target in a transgenic yeast system by replacing the halofuginone-insensitive yeast homolog *Sc*PRS with wild-type and mutant *Pf*cPRS, which yielded halofuginone-sensitive and halofuginone-insensitive strains, respectively. Separately, wild-type and mutant *Pf*cPRS were purified and biochemically characterized to confirm *Pf*cPRS as a molecular target of halofuginone

analogs, and functional validation led to identification of resistance mutations. In addition, molecular dynamics simulations were performed to provide a mechanistic rationale for the identified resistance mutations and the lack of affinity of halofuginone for yeast PRS. All in vitro experiments were repeated at least twice. Finally, halofuginone and the modified analog halofuginol were evaluated in mice for efficacy against liver- and blood-stage malaria. Mice were infected and randomized into different groups before drug treatment. Investigators were not blinded for animal allocation, compound administration, and clinical evaluation of mice or collected tissues.

All in vivo protocols were approved by the Animal Care Committee of the Instituto de Medicina Molecular, University of Lisbon, and were performed according to the regulations of the European guidelines 86/609/EEG. Guidelines for humane endpoints were strictly followed for all in vivo experiments.

### Statistical analysis

Statistical analyses were performed in Prism 6.0 (GraphPad Software Inc.). Data are shown as means ± SD. Analytical tests for statistical significance and *P* values are specified in each figure legend. $EC_{50}$ values were calculated using a four-parameter nonlinear regression curve fit. Ordinary one-way ANOVA (Sidak's multiple comparison test) was used for comparison of three or more groups. Mann-Whitney test was used for two groups. For survival data, the Kaplan-Meier method and log-rank test (Mantel-Cox test) were used for comparisons between groups.

## SUPPLEMENTARY MATERIALS

www.sciencetranslationalmedicine.org/cgi/content/full/7/288/288ra77/DC1
Materials and Methods
Fig. S1. High-resolution melt assay of *Pf*cPRS identifies mutant loci.
Fig. S2. Halofuginone is not cross-resistant with common anti-antimalarials.
Fig. S3. Proline-dependent sensitivity of *P. falciparum* to halofuginone.
Fig. S4. Transgenic *S. cerevisiae* expressing wild-type *Pf*cPRS is sensitive to halofuginone.
Fig. S5. Proline-dependent sensitivity of transgenic *S. cerevisiae* to halofuginone.
Fig. S6. AAR pathway.
Fig. S7. Quantification of p-eIF2α protein in Fig. 2C.
Fig. S8. Multiple protein sequence alignment of the class II core domains of proline tRNA synthetases from diverse species.
Fig. S9. Comparison of molecular dynamics models comparing the impact of the L482F and L482H mutations in *Pf*cPRS.
Fig. S10. Proposed mechanism for halofuginone epimerization.
Fig. S11. Sensitivity of *S. cerevisiae* model strains to halofuginone.
Fig. S12. Induction of eIF2α phosphorylation by halofuginol.
Fig. S13. Necropsy of halofuginol and vehicle-treated mice.
Fig. S14. In vivo potency of halofuginone in liver-stage *P. berghei* infection model.
Table S1. $EC_{50}$ values of febrifugine and analogs for erythrocytic-stage 3D7, Dd2 wild-type, and Dd2 halofuginone-resistant *P. falciparum* strains.
Table S2. Source data for Fig. 5A.
Table S3. Source data for Fig. 5B.
Table S4. Source data for Fig. 5C.
Table S5. Source data for fig. S14.
References (*44*–*70*)

## REFERENCES AND NOTES


1. World Health Organization, *World Health Statistics 2012* (World Health Organization, Geneva, Switzerland, 2012).
2. F. Ariey, B. Witkowski, C. Amaratunga, J. Beghain, A.-C. Langlois, N. Khim, S. Kim, V. Duru, C. Bouchier, L. Ma, P. Lim, R. Leang, S. Duong, S. Sreng, S. Suon, C. M. Chuor, D. M. Bout, S. Ménard, W. O. Rogers, B. Genton, T. Fandeur, O. Miotto, P. Ringwald, J. Le Bras, A. Berry, J. C. Barale, R. M. Fairhurst, F. Benoit-Vical, O. Mercereau-Puijalon, D. Ménard, A molecular marker of artemisinin-resistant *Plasmodium falciparum* malaria. *Nature* **505**, 50–55 (2014).
3. C. Wongsrichanalai, S. R. Meshnick, Declining artesunate-mefloquine efficacy against falciparum malaria on the Cambodia-Thailand border. *Emerg. Infect. Dis.* **14**, 716–719 (2008).
4. D. A. Fidock, P. J. Rosenthal, S. L. Croft, R. Brun, S. Nwaka, Antimalarial drug discovery: Efficacy models for compound screening. *Nat. Rev. Drug Discov.* **3**, 509–520 (2004).
5. P. L. Alonso, G. Brown, M. Arevalo-Herrera, F. Binka, C. Chitnis, F. Collins, O. K. Doumbo, B. Greenwood, B. F. Hall, M. M. Levine, K. Mendis, R. D. Newman, C. V. Plowe, M. H. Rodriguez, R. Sinden, L. Slutsker, M. Tanner, A research agenda to underpin malaria eradication. *PLOS Med.* **8**, e1000406 (2011).
6. A. Nilsen, A. N. LaCrue, K. L. White, I. P. Forquer, R. M. Cross, J. Marfurt, M. W. Mather, M. J. Delves, D. M. Shackleford, F. E. Saenz, J. M. Morrisey, J. Steuten, T. Mutka, Y. Li, G. Wirjanata, E. Ryan, S. Duffy, J. X. Kelly, B. F. Sebayang, A.-M. Zeeman, R. Noviyanti, R. E. Sinden, C. H. M. Kocken, R. N. Price, V. M. Avery, I. Angulo-Barturen, M. B. Jiménez-Díaz, S. Ferrer, E. Herreros, L. M. Sanz, F. J. Gamo, I. Bathurst, J. N. Burrows, P. Siegl, R. K. Guy, R. W. Winter, A. B. Vaidya, S. A. Charman, D. E. Kyle, R. Manetsch, M. K. Riscoe, Quinolone-3-diarylethers: A new class of antimalarial drug. *Sci. Transl. Med.* **5**, 177ra37 (2013).
7. T. L. Keller, D. Zocco, M. S. Sundrud, M. Hendrick, M. Edenius, J. Yum, Y.-J. Kim, H.-K. Lee, J. F. Cortese, D. F. Wirth, J. D. Dignam, A. Rao, C.-Y. Yeo, R. Mazitschek, M. Whitman, Halofuginone and other febrifugine derivatives inhibit prolyl-tRNA synthetase. *Nat. Chem. Biol.* **8**, 311–317 (2012).
8. J. S. Pham, R. Sakaguchi, L. M. Yeoh, N. S. De Silva, G. I. McFadden, Y.-M. Hou, S. A. Ralph, A dual-targeted aminoacyl-tRNA synthetase in *Plasmodium falciparum* charges cytosolic and apicoplast $tRNA^{Cys}$. *Biochem. J.* **458**, 513–523 (2014).
9. K. E. Jackson, S. Habib, M. Frugier, R. Hoen, S. Khan, J. S. Pham, L. Ribas de Pouplana, M. Royo, M. A. Santos, A. Sharma, S. A. Ralph, Protein translation in *Plasmodium* parasites. *Trends Parasitol.* **27**, 467–476 (2011).
10. S. Khan, A. Sharma, A. Jamwal, V. Sharma, A. K. Pole, K. K. Thakur, A. Sharma, Uneven spread of *cis*- and *trans*-editing aminoacyl-tRNA synthetase domains within translational compartments of *P. falciparum*. *Sci. Rep.* **1**, 188 (2011).
11. Y.-K. Zhang, J. J. Plattner, Y. R. Freund, E. E. Easom, Y. Zhou, L. Ye, H. Zhou, D. Waterson, F.-J. Gamo, L. M. Sanz, M. Ge, Z. Li, L. Li, H. Wang, H. Cui, Benzoxaborole antimalarial agents. Part 2: Discovery of fluoro-substituted 7-(2-carboxyethyl)-1,3-dihydro-1-hydroxy-2,1-benzoxaboroles. *Bioorg. Med. Chem. Lett.* **22**, 1299–1307 (2012).
12. K. E. Jackson, J. S. Pham, M. Kwek, N. S. De Silva, S. M. Allen, C. D. Goodman, G. I. McFadden, L. Ribas de Pouplana, S. A. Ralph, Dual targeting of aminoacyl-tRNA synthetases to the apicoplast and cytosol in *Plasmodium falciparum*. *Int. J. Parasitol.* **42**, 177–186 (2012).
13. E. S. Istvan, N. V. Dharia, S. E. Bopp, I. Gluzman, E. A. Winzeler, D. E. Goldberg, Validation of isoleucine utilization targets in *Plasmodium falciparum*. *Proc. Natl. Acad. Sci. U.S.A.* **108**, 1627–1632 (2011).
14. D. Hoepfner, C. W. McNamara, C. S. Lim, C. Studer, R. Riedl, T. Aust, S. L. McCormack, D. M. Plouffe, S. Meister, S. Schuierer, U. Plikat, N. Hartmann, F. Staedtler, S. Cotesta, E. K. Schmitt, F. Petersen, F. Supek, R. J. Glynne, J. A. Tallarico, J. A. Porter, M. C. Fishman, C. Bodenreider, T. T. Diagana, N. R. Movva, E. A. Winzeler, Selective and specific inhibition of the *Plasmodium falciparum* lysyl-tRNA synthetase by the fungal secondary metabolite cladosporin. *Cell Host Microbe* **11**, 654–663 (2012).
15. I. M. Tonkin, T. S. Work, A new antimalarial drug. *Nature* **156**, 630 (1945).
16. W. R. Burns, East meets West: How China almost cured malaria. *Endeavour* **32**, 101–106 (2008).
17. S. Jiang, Q. Zeng, M. Gettayacamin, A. Tungtaeng, S. Wannaying, A. Lim, P. Hansukjariya, C. O. Okunji, S. Zhu, D. Fang, Antimalarial activities and therapeutic properties of febrifugine analogs. *Antimicrob. Agents Chemother.* **49**, 1169–1176 (2005).
18. M. Guo, P. Schimmel, Essential nontranslational functions of tRNA synthetases. *Nat. Chem. Biol.* **9**, 145–153 (2013).
19. T. K. Bhatt, C. Kapil, S. Khan, M. A. Jairajpuri, V. Sharma, D. Santoni, F. Silvestrini, E. Pizzi, A. Sharma, A genomic glimpse of aminoacyl-tRNA synthetases in malaria parasite *Plasmodium falciparum*. *BMC Genomics* **10**, 644 (2009).
20. D. J. Park, A. K. Lukens, D. E. Neafsey, S. F. Schaffner, H.-H. Chang, C. Valim, U. Ribacke, D. Van Tyne, K. Galinsky, M. Galligan, J. S. Becker, D. Ndiaye, S. Mboup, R. C. Wiegand, D. L. Hartl, P. C. Sabeti, D. F. Wirth, S. K. Volkman, Sequence-based association and selection scans identify drug resistance loci in the *Plasmodium falciparum* malaria parasite. *Proc. Natl. Acad. Sci. U.S.A.* **109**, 13052–13057 (2012).
21. E. L. Flannery, D. A. Fidock, E. A. Winzeler, Using genetic methods to define the targets of compounds with antimalarial activity. *J. Med. Chem.* **56**, 7761–7771 (2013).
22. C. K. Dong, S. Urgaonkar, J. F. Cortese, F.-J. Gamo, J. F. Garcia-Bustos, M. Lafuente, V. Patel, L. Ross, B. I. Coleman, E. Derbyshire, C. B. Clish, A. E. Serrano, M. Cromwell, R. H. Barker, J. D. Dvorin, M. T. Duraisingh, D. F. Wirth, J. Clardy, R. Mazitschek, Identification and validation of tetracyclic benzothiazepines as *Plasmodium falciparum* cytochrome $bc_1$ inhibitors. *Chem. Biol.* **18**, 1602–1610 (2011).
23. H. Li, B. Handsaker, A. Wysoker, T. Fennell, J. Ruan, N. Homer, G. Marth, G. Abecasis, R. Durbin; 1000 Genome Project Data Processing Subgroup, The Sequence Alignment/Map format and SAMtools. *Bioinformatics* **25**, 2078–2079 (2009).

24. A. McKenna, M. Hanna, E. Banks, A. Sivachenko, K. Cibulskis, A. Kernytsky, K. Garimella, D. Altshuler, S. Gabriel, M. Daly, M. A. DePristo, The Genome Analysis Toolkit: A MapReduce framework for analyzing next-generation DNA sequencing data. *Genome Res.* **20**, 1297–1303 (2010).
25. R. Daniels, D. Ndiaye, M. Wall, J. McKinney, P. D. Séne, P. C. Sabeti, S. K. Volkman, S. Mboup, D. F. Wirth, Rapid, field-deployable method for genotyping and discovery of single-nucleotide polymorphisms associated with drug resistance in *Plasmodium falciparum*. *Antimicrob. Agents Chemother.* **56**, 2976–2986 (2012).
26. C. Aurrecoechea, J. Brestelli, B. P. Brunk, J. Dommer, S. Fischer, B. Gajria, X. Gao, A. Gingle, G. Grant, O. S. Harb, M. Heiges, F. Innamorato, J. Iodice, J. C. Kissinger, E. Kraemer, W. Li, J. A. Miller, V. Nayak, C. Pennington, D. F. Pinney, D. S. Roos, C. Ross, C. J. Stoeckert Jr., C. Treatman, H. Wang, PlasmoDB: A functional genomic database for malaria parasites. *Nucleic Acids Res.*, **37**, D539–D543 (2009).
27. M. S. Sundrud, S. B. Koralov, M. Feuerer, D. P. Calado, A. E. Kozhaya, A. Rhule-Smith, R. E. Lefebvre, D. Unutmaz, R. Mazitschek, H. Waldner, M. Whitman, T. Keller, A. Rao, Halofuginone inhibits $T_H17$ cell differentiation by activating the amino acid starvation response. *Science* **324**, 1334–1338 (2009).
28. A. G. Hinnebusch, Translational regulation of GCN4 and the general amino acid control of yeast. *Annu. Rev. Microbiol.* **59**, 407–450 (2005).
29. C. Fennell, S. Babbitt, I. Russo, J. Wilkes, L. Ranford-Cartwright, D. E. Goldberg, C. Doerig, PfeIK1, a eukaryotic initiation factor 2α kinase of the human malaria parasite *Plasmodium falciparum*, regulates stress-response to amino-acid starvation. *Malar. J.* **8**, 99 (2009).
30. H. Zhou, L. Sun, X.-L. Yang, P. Schimmel, ATP-directed capture of bioactive herbal-based medicine on human tRNA synthetase. *Nature* **494**, 121–124 (2013).
31. V. Jain, H. Kikuchi, Y. Oshima, A. Sharma, M. Yogavel, Structural and functional analysis of the anti-malarial drug target prolyl-tRNA synthetase. *J. Struct. Funct. Genomics* **15**, 181–190 (2014).
32. J. Son, E. H. Lee, M. Park, J. H. Kim, J. Kim, S. Kim, Y. H. Jeon, K. Y. Hwang, Conformational changes in human prolyl-tRNA synthetase upon binding of the substrates proline and ATP and the inhibitor halofuginone. *Acta Crystallogr. D Biol. Crystallogr.* **69**, 2136–2145 (2013).
33. Y. Takeuchi, M. Oshige, K. Azuma, H. Abe, T. Harayama, Concise synthesis of *dl*-febrifugine. *Chem. Pharm. Bull.* **53**, 868–869 (2005).
34. H. Kikuchi, H. Tasaka, S. Hirai, Y. Takaya, Y. Iwabuchi, H. Ooi, S. Hatakeyama, H.-S. Kim, Y. Wataya, Y. Oshima, Potent antimalarial febrifugine analogues against the *Plasmodium* malaria parasite. *J. Med. Chem.* **45**, 2563–2570 (2002).
35. M. R. Linder, A. R. Heckeroth, M. Najdrowski, A. Daugschies, D. Schollmeyer, C. Miculka, (2*R*,3*S*)-(+)- and (2*S*,3*R*)-(−)-Halofuginone lactate: Synthesis, absolute configuration, and activity against *Cryptosporidium parvum*. *Bioorg. Med. Chem. Lett.* **17**, 4140–4143 (2007).
36. E. R. Derbyshire, R. Mazitschek, J. Clardy, Characterization of *Plasmodium* liver stage inhibition by halofuginone. *ChemMedChem* **7**, 844–849 (2012).
37. W. Peters, The chemotherapy of rodent malaria, XXII. The value of drug-resistant strains of *P. berghei* in screening for blood schizontocidal activity. *Ann. Trop. Med. Parasitol.* **69**, 155–171 (1975).
38. K. K. Hanson, A. S. Ressurreição, K. Buchholz, M. Prudêncio, J. D. Herman-Ornelas, M. Rebelo, W. L. Beatty, D. F. Wirth, T. Hänscheid, R. Moreira, M. Marti, M. M. Mota, Torins are potent antimalarials that block replenishment of *Plasmodium* liver stage parasitophorous vacuole membrane proteins. *Proc. Natl. Acad. Sci. U.S.A.* **110**, E2838–E2847 (2013).
39. E. L. Flannery, A. K. Chatterjee, E. A. Winzeler, Antimalarial drug discovery—Approaches and progress toward new medicines. *Nat. Rev. Microbiol.* **11**, 849–862 (2013).
40. N. Valbuena, A. E. Rozalén, S. Moreno, Fission yeast TORC1 prevents eIF2α phosphorylation in response to nitrogen and amino acids via Gcn2 kinase. *J. Cell Sci.* **125**, 5955–5959 (2012).
41. L. A. Trotz-Williams, B. D. Jarvie, A. S. Peregrine, T. F. Duffield, K. E. Leslie, Efficacy of halofuginone lactate in the prevention of cryptosporidiosis in dairy calves. *Vet. Rec.* **168**, 509 (2011).
42. M. Naciri, R. Mancassola, P. Yvoré, J. E. Peeters, The effect of halofuginone lactate on experimental *Cryptosporidium parvum* infections in calves. *Vet. Parasitol.* **45**, 199–207 (1993).
43. D.-F. Zhang, B.-B. Sun, Y.-Y. Yue, H.-J. Yu, H.-L. Zhang, Q.-J. Zhou, A.-F. Du, Anticoccidial effect of halofuginone hydrobromide against *Eimeria tenella* with associated histology. *Parasitol. Res.* **111**, 695–701 (2012).
44. W. Trager, J. B. Jensen, Human malaria parasites in continuous culture. *Science* **193**, 673–675 (1976).
45. M. Smilkstein, N. Sriwilaijaroen, J. X. Kelly, P. Wilairat, M. Riscoe, Simple and inexpensive fluorescence-based technique for high-throughput antimalarial drug screening. *Antimicrob. Agents Chemother.* **48**, 1803–1806 (2004).
46. T. N. Bennett, M. Paguio, B. Gligorijevic, C. Seudieu, A. D. Kosar, E. Davidson, P. D. Roepe, Novel, rapid, and inexpensive cell-based quantification of antimalarial drug efficacy. *Antimicrob. Agents Chemother.* **48**, 1807–1810 (2004).
47. V. Rosario, Cloning of naturally occurring mixed infections of malaria parasites. *Science* **212**, 1037–1038 (1981).
48. J. Narasimhan, B. R. Joyce, A. Naguleswaran, A. T. Smith, M. R. Livingston, S. E. Dixon, I. Coppens, R. C. Wek, W. J. Sullivan Jr., Translation regulation by eukaryotic initiation factor-2 kinases in the development of latent cysts in *Toxoplasma gondii*. *J. Biol. Chem.* **283**, 16591–16601 (2008).
49. Y. Hu, A. Rolfs, B. Bhullar, T. V. S. Murthy, C. Zhu, M. F. Berger, A. A. Camargo, F. Kelley, S. McCarron, D. Jepson, A. Richardson, J. Raphael, D. Moreira, E. Taycher, D. Zuo, S. Mohr, M. F. Kane, J. Williamson, A. Simpson, M. L. Bulyk, E. Harlow, G. Marsischky, R. D. Kolodner, J. LaBaer, Approaching a complete repository of sequence-verified protein-encoding clones for *Saccharomyces cerevisiae*. *Genome Res.* **17**, 536–543 (2007).
50. S. Alberti, A. D. Gitler, S. Lindquist, A suite of Gateway cloning vectors for high-throughput genetic analysis in *Saccharomyces cerevisiae*. *Yeast* **24**, 913–919 (2007).
51. R. D. Gietz, R. A. Woods, Transformation of yeast by lithium acetate/single-stranded carrier DNA/polyethylene glycol method. *Methods Enzymol.* **350**, 87–96 (2002).
52. F. M. Ausubel, R. Brent, R. E. Kingston, D. Moore, J. G. Seidman, K. Struhl, *Current Protocols in Molecular Biology* (John Wiley & Sons Inc., Hoboken, NJ, 2004).
53. U. Gueldener, J. Heinisch, G. J. Koehler, D. Voss, J. H. Hegemann, A second set of *loxP* marker cassettes for Cre-mediated multiple gene knockouts in budding yeast. *Nucleic Acids Res.* **30**, e23 (2002).
54. A. L. Goldstein, J. H. McCusker, Three new dominant drug resistance cassettes for gene disruption in *Saccharomyces cerevisiae*. *Yeast* **15**, 1541–1553 (1999).
55. I. H. J. Ploemen, M. Prudêncio, B. G. Douradinha, J. Ramesar, J. Fonager, G.-J. van Gemert, A. J. F. Luty, C. C. Hermsen, R. W. Sauerwein, F. G. Baptista, M. M. Mota, A. P. Waters, I. Que, C. W. Lowik, S. M. Khan, C. J. Janse, B. M. D. Franke-Fayard, Visualisation and quantitative analysis of the rodent malaria liver stage by real time imaging. *PLOS One* **4**, e7881 (2009).
56. M. P. Jacobson, D. L. Pincus, C. S. Rapp, T. J. F. Day, B. Honig, D. E. Shaw, R. A. Friesner, A hierarchical approach to all-atom protein loop prediction. *Proteins* **55**, 351–367 (2004).
57. R. A. Friesner, R. B. Murphy, M. P. Repasky, L. L. Frye, J. R. Greenwood, T. A. Halgren, P. C. Sanschagrin, D. T. Mainz, Extra precision glide: Docking and scoring incorporating a model of hydrophobic enclosure for protein–ligand complexes. *J. Med. Chem.* **49**, 6177–6196 (2006).
58. R. A. Friesner, J. L. Banks, R. B. Murphy, T. A. Halgren, J. J. Klicic, D. T. Mainz, M. P. Repasky, E. H. Knoll, M. Shelley, J. K. Perry, D. E. Shaw, P. Francis, P. S. Shenkin, Glide: A new approach for rapid, accurate docking and scoring. 1. Method and assessment of docking accuracy. *J. Med. Chem.* **47**, 1739–1749 (2004).
59. G. Estiu, N. West, R. Mazitschek, E. Greenberg, J. E. Bradner, O. Wiest, On the inhibition of histone deacetylase 8. *Bioorg. Med. Chem.* **18**, 4103–4110 (2010).
60. D. A. Case, T. A. Darden, T. E. Cheatham III, C. L. Simmerling, J. Wang, R. E. Duke, R. Luo, M. Crowley, R. C. Walker, W. Zhang, *AMBER 10* (University of California, San Francisco, 2008).
61. W. L. Jorgensen, J. Chandrasekhar, J. D. Madura, R. W. Impey, M. L. Klein, Comparison of simple potential functions for simulating liquid water. *J. Chem. Phys.* **79**, 926 (1983).
62. C. Schafmeister, W. S. Ross, V. Romanovski, *LEaP* (University of California, San Francisco, 1995).
63. J. Wang, R. M. Wolf, J. W. Caldwell, P. A. Kollman, D. A. Case, Development and testing of a general amber force field. *J. Comput. Chem.* **25**, 1157–1174 (2004).
64. J. Wang, W. Wang, P. A. Kollman, D. A. Case, Automatic atom type and bond type perception in molecular mechanical calculations. *J. Mol. Graph. Model.* **25**, 247–260 (2006).
65. T. Fox, P. A. Kollman, Application of the resp methodology in the parametrization of organic solvents. *J. Phys. Chem. B* **102**, 8070–8079 (1998).
66. J.-P. Ryckaert, G. Ciccotti, H. J. C. Berendsen, Numerical integration of the cartesian equations of motion of a system with constraints: Molecular dynamics of *n*-alkanes. *J. Comput. Phys.* **23**, 327–341 (1977).
67. R. Pastor, B. Brooks, A. Szabo, An analysis of the accuracy of Langevin and molecular dynamics algorithms. *Mol. Phys.* **65**, 1409–1419 (1988).
68. U. Essmann, L. Perera, M. L. Berkowitz, T. Darden, H. Lee, L. G. Pedersen, A smooth particle mesh Ewald method. *J. Chem. Phys.* **103**, 8577 (1995).
69. H. G. Petersen, Accuracy and efficiency of the particle mesh Ewald method. *J. Chem. Phys.* **103**, 3668 (1995).
70. A. Marchler-Bauer, S. Lu, J. B. Anderson, F. Chitsaz, M. K. Derbyshire, C. DeWeese-Scott, J. H. Fong, L. Y. Geer, R. C. Geer, N. R. Gonzales, M. Gwadz, D. I. Hurwitz, J. D. Jackson, Z. Ke, C. J. Lanczycki, F. Lu, G. H. Marchler, M. Mullokandov, M. V. Omelchenko, C. L. Robertson, J. S. Song, N. Thanki, R. A. Yamashita, D. Zhang, N. Zhang, C. Zheng, S. H. Bryant, CDD: A Conserved Domain Database for the functional annotation of proteins. *Nucleic Acids Res.* **39**, D225–D229 (2011).


**Acknowledgments:** We would like to acknowledge R. Daniels for advice on assay design and experimental guidance. **Funding:** We gratefully acknowledge financial support from the Gates Foundation (D.F.W. and R.M., OPP1086203), the NIH (D.F.W.) AI105786 (W.J.S.), 5F32AI084440-02 (L.R.P.), CA92577 (P.S.), and GM099796 (E.R.D.), the Center for Rare and Neglected Diseases at the University of Notre Dame (O.W. and G.E.), generous allocation of computing resources by the NSF through TeraGrid grant TG-CHE090124 (O.W.), a fellowship from the National Foundation for Cancer Research (P.S.), SFRH/BD/80162/2011 (S.A.S.), PTDC/SAU-MIC/113697/2009 (V.Z.-L.), and EXCL/IMI-MIC/0056/2012 (M.M.M.) (Fundação para a Ciência e Tecnologia, Portugal), Howard Hughes Medical Institute (S.L.), and start-up funding provided by the Center for Systems Biology, Massachusetts General Hospital (R.M.). **Author contributions:** J.D.H., L.R.P., A.K.L., S.E.B., D.F.W., and R.M. wrote the manuscript; D.F.W. and R.M. designed the study with input from J.D.H. and

L.R.P.; J.D.H. performed in vitro blood-stage *Plasmodium* culture experiments (resistance selection, drug profiling, mechanistic studies, PCR, and Western blot analysis); L.R.P. performed all yeast-related experiments; J.F.C. performed selection experiments; G.E. performed modeling studies; K.G. performed sequencing analysis; V.Z.-L. performed all in vivo studies; E.R.D. performed in vitro liver-stage assays; U.R., V.P., A.K.L., and S.E.B assisted with in vitro blood-stage *Plasmodium* culture experiments; C.B.C. performed mass spectrometry analysis; H.Z. expressed and purified recombinant protein and performed biochemical assays; M.W. performed cytotoxicity assays; and R.M. and S.A.S. designed, synthesized, and characterized small-molecule inhibitors. J.D.H., L.R.P., G.E., K.G., V.Z.-L, C.B.C., H.Z., P.S., S.L., M.M.M., O.W., D.F.W., and R.M. analyzed data; W.J.S. contributed reagents; and W.J.S., P.S., S.L., J.C., M.M.M., T.L.K., M.W., O.W., D.F.W., and R.M. provided scientific leadership. **Competing interests:** R.M. is a consultant to Acetylon Pharmaceuticals and ERX Pharmaceuticals, and a member of the advisory board of Malaria Free World; D.F.W. serves on the board of the Burroughs Wellcome Fund and the Marine Biological Lab; J.C. is consultant to Warp Drive Bio; S.L. is a member on the Board of Directors of Johnson & Johnson and consultant to Yumanity; and C.B.C. is consultant to Agios Pharmaceuticals, Capital Royalty, SynapDx Corp., and General Metabolics. The following patent applications have been filed by Harvard University: PCT/US2008/61188740 and PCT/US2012/61586271. The other authors declare that they have no competing interests. **Data and materials availability:** The sequencing reads were deposited in National Center for Biotechnology Information (NCBI) Sequence Read Archive (SRA) (http://www.ncbi.nlm.nih.gov/Traces/sra/) under SRX110289 (HFGR-I) and SRX158283 (HFGR-II).

Submitted 23 November 2014
Accepted 1 May 2015
Published 20 May 2015
10.1126/scitranslmed.aaa3575

**Citation:** J. D. Herman, L. R. Pepper, J. F. Cortese, G. Estiu, K. Galinsky, V. Zuzarte-Luis, E. R. Derbyshire, U. Ribacke, A. K. Lukens, S. A. Santos, V. Patel, C. B. Clish, W. J. Sullivan Jr., H. Zhou, S. E. Bopp, P. Schimmel, S. Lindquist, J. Clardy, M. M. Mota, T. L. Keller, M. Whitman, O. Wiest, D. F. Wirth, R. Mazitschek, The cytoplasmic prolyl-tRNA synthetase of the malaria parasite is a dual-stage target of febrifugine and its analogs. *Sci. Transl. Med.* **7**, 288ra77 (2015).

Science Translational Medicine
AAAS

# The cytoplasmic prolyl-tRNA synthetase of the malaria parasite is a dual-stage target of febrifugine and its analogs

Jonathan D. Herman *et al.*

*Sci Transl Med* **7**, 288ra77 (2015);
DOI: 10.1126/scitranslmed.aaa3575

Editor's Summary

## An ancient remedy for a modern scourge

Malaria is a devastating disease. It is caused by a unicellular parasite and claims more than 600,000 lives every year —mostly young children and pregnant women. Renewed worldwide efforts to eradicate malaria demand new therapeutic approaches to overcome the emergence and spread of clinical resistance to mainstay drugs.

Now, Herman *et al*. validate the cytoplasmic prolyl-tRNA synthetase of the *Plasmodium* malaria parasite as the enigmatic target of the natural plant product febrifugine, the active principle of an ancient herbal malaria remedy that has been used for millennia in China. These authors establish a path forward for the rational development of next-generation antimalarial therapies based on febrifugine and its analogs.



*Science Translational Medicine* (print ISSN 1946-6234; online ISSN 1946-6242) is published weekly, except the last week in December, by the American Association for the Advancement of Science, 1200 New York Avenue NW, Washington, DC 20005. 